

Review

Commercial Nanoparticles for Stem Cell Labeling and Tracking

Yaqi Wang¹✉, Chenjie Xu²✉, Hooisweng Ow¹

1. Hybrid Silica Technologies, Cambridge, Massachusetts, USA 02139.
2. Division of Bioengineering, School of Chemical and Biomedical Engineering, Nanyang Technological University, Singapore 637457.

✉ Corresponding authors: Email: yaqiw@hybridsilica.com, cjxu@ntu.edu.sg.

© Ivyspring International Publisher. This is an open-access article distributed under the terms of the Creative Commons License (<http://creativecommons.org/licenses/by-nc-nd/3.0/>). Reproduction is permitted for personal, noncommercial use, provided that the article is in whole, unmodified, and properly cited.

Received: 2012.11.30; Accepted: 2013.02.03; Published: 2013.07.20

Abstract

Stem cell therapy provides promising solutions for diseases and injuries that conventional medicines and therapies cannot effectively treat. To achieve its full therapeutic potentials, the homing process, survival, differentiation, and engraftment of stem cells post transplantation must be clearly understood. To address this need, non-invasive imaging technologies based on nanoparticles (NPs) have been developed to track transplanted stem cells. Here we summarize existing commercial NPs which can act as contrast agents of three commonly used imaging modalities, including fluorescence imaging, magnetic resonance imaging and photoacoustic imaging, for stem cell labeling and tracking. Specifically, we go through their technologies, industry distributors, applications and existing concerns in stem cell research. Finally, we provide an industry perspective on the potential challenges and future for the development of new NP products.

Key words: stem cell, cell therapy, commercial nanoparticle, tracking, imaging, industry.

1. Introduction

Cell therapy is an expanding research area since the first successful syngeneic bone marrow transplant in two patients in 1956.¹ It provides promising solutions for diseases and injuries that conventional medicines and therapies cannot effectively treat with the fact that cells can perform better physiologic and metabolic duties than any mechanical device, recombinant protein or chemical compound.² Extensive research has been focused on the replacement and restoration of functional damaged or diseased tissues through cell transplantation, in particular, stem and progenitor cells.³ To achieve their therapeutic potentials, stem cells must home to the site of injury/disease, differentiate into the target cells, survive, and engraft after transplantation.⁴ However, comprehensive understanding of the above mentioned information is still lacking, which results in contradictory results in recent clinical trials.⁵ Therefore,

there is an urgent need to better understand the homing process, survival, distribution, and engraftment of transplanted cells.³

To meet this need, non-invasive imaging technologies based on nanoparticles (NPs) have been developed to replace the traditional invasive histological analysis.⁶⁻¹⁴ Initially being produced in research laboratories, NPs have been undergoing fast commercialization and become standardized products in the recent years.¹⁶ Given the reasonable cost, easy accessibility, and the non-invasiveness, fluorescent imaging, magnetic resonance imaging (MRI), and photoacoustic imaging are currently the most favorable imaging modalities for the application of cell tracking. This trend of using commercially available NPs should allow the standardization of the procedure in the labeling and tracking of cells, which will improve the repeatability and adherence to the requirements of

safety regulatory body.

In this review, after a brief discussion of the common imaging modalities used in stem cell tracking, we summarize the commercially available NPs, which have been or could potentially be used for the labeling and tracking of stem cells. Specifically, we focus on those NPs that act as contrast agents for fluorescent imaging, MRI, or photoacoustic imaging. Finally, we also discuss the concerns of existing NP products and the future of development of new NP products for stem cell tracking.

2. Commonly used imaging modalities for stem cells tracking with NPs

Commonly used imaging modalities for stem cells tracking with NPs include fluorescence imaging, magnetic resonance imaging (MRI), photoacoustic imaging and nuclear imaging using radioactive isotopes.

Fluorescent imaging provides good sensitivity and is able to image and track cell activities and biological phenomena at cellular level.¹⁶⁻²⁰ In traditional fluorescent imaging, cell imaging and tracking are based on fluorescent dye molecules, which are restricted to broad emission spectrum, limited emission per molecule and unsatisfactory photostability.²¹ NPs overcome these disadvantages by offering stronger and more stable fluorescence.²¹

MRI is a fast, non-invasive, deep tissue penetrating technique^{3, 22} which provides good contrast between the different soft tissues of the body, and reconstructs 2D or 3D images of the tissues. NPs improve the sensitivity and detectability of the objects in MRI through shortening the T1/T1* or T2/T2* relaxation time²², which further advances the use of the MRI technique in cell imaging and tracking.

Photoacoustic imaging is a non-invasive hybrid imaging technique which provides the advantages of the high contrast of optics and the high resolution of acoustic and is capable of visualizing morphological, functional and molecular properties.²⁷ Thus photoacoustic imaging has great potential for *in vivo* longitudinal tracking of stem cells. However, stem cells don't have sufficient optical absorption coefficient and cannot be visualized directly by photoacoustic imaging technique.²⁷ NP-based contrast agents are used to label stem cells to create sufficient detectable acoustic source.²⁷

Positron emission tomography (PET) and single-photo emission computed tomography (SPECT) are nuclear imaging techniques utilizing radioactive isotopes. PET and SPECT collect gamma rays to reconstruct 3D images of the samples. Both techniques are suitable for deep tissue imaging and can provide

assessment of cell viability or function.³ However, radioactive isotopes usually have short half-lives, which limit their applications in long term imaging and cell tracking.³ Furthermore, the accessibility of isotopes and the safety issue have restricted their applications. NPs for PET or SPECT are usually pre-synthesized polymer NPs (e.g latex beads ²⁸), inorganic NPs (e.g. quantum dots (QDs) ²⁹, magnetite NPs ³⁰, gold NPs ³¹) or lipid NP ³² chelating radioactive isotopes. There are currently no commercial NPs labeled with radioactive isotopes.

3. Commercial fluorescent NPs for stem cell labeling and tracking

Fluorescence imaging provides high sensitivity, high resolution, and possibility to monitor biological phenomena in real time ^{3,33} They are also attractive in terms of cost, accessibility, and visualization. Thus fluorescence imaging is the most widely used modality in tracking stem cells. Fluorescent NP products on the market are mainly fluorescent polymer NP, quantum dots and fluorescent silica NPs.

3.1 Fluorescent polymer NPs.

Polymer NPs are generally prepared through the dispersion of preformed polymers or polymerization of monomers.³⁴ A number of techniques within the scope include solvent evaporation, salting-out, dialysis, supercritical fluid technology, emulsion, surfactant-free emulsion, and interfacial polymerization. To become fluorescent, organic dyes could be either physically entrapped in the polymer interior during the preparation of NPs or covalently bound to the polymer chain before the preparation of NPs.³⁵ Fluorescent polymer NPs can be examined with an epi-fluorescence microscope, confocal microscope, fluorometer, fluorescence spectrophotometer, or fluorescence activated cell sorter.

Currently, the most common fluorescent polymer NPs are polystyrene (PS) NPs, which are distributed by all the major life science and biotechnology companies, such as Sigma-Aldrich, Thermo-Fisher and Invitrogen. They are mainly prepared through the emulsion polymerization.³⁶ Existing products are available with the form of non-modified, sulfate-modified, aldehyde-modified, carboxylate-modified or amine-modified surface, and supplied as 0.5-5% aqueous suspension with trace amount of surfactant to aid dispersion and prevent aggregation. Despite the wide applications, PS NPs suffer from low dye incorporation and inadequate dye molecule protection, which result in dye leaching, quenching and photobleaching.³⁵ To address this problem, Duke scientific and Thermo fisher utilize

Firefli™ developed internally-dyed PS NPs which incorporate the dye throughout the polymer matrix.³⁷ On another hand, Sigma-Aldrich provides 40nm PD fluorescent polymer NPs made of polymer similar to polystyrene, but has reduced oxygen permeability, which results in a higher photo-stability for most dyes.³⁹ FluoSpheres® beads from Molecular Probes® (Invitrogen) are ultra clean, intense fluorescent latex particles that typically show little or no photo bleaching, even when excited with the intense illumination. In addition to PS, fluorescent polymer NPs could also be made of conjugated fluorescent polymers which exhibit amplified fluorescence responses, such as poly(arylenediethylenes),⁴⁰ poly(3,4-ethylenedioxy-thiophene),⁴¹ poly(thiophene-3-yl-acetic

acid),⁴² and polyacetylene.⁴³ Table 1 lists the main existing products of fluorescent polymer NPs on the market, including the specifications, brand names and distributors. The fluorescence properties in Table 1 are provided by manufactures for references only. We must note that all the commercial fluorescent NPs listed in Table 1 are polymer NPs encapsulating dyes in their polymer matrices. There is no conjugated fluorescent polymer NP product, although researches show that conjugated polymers have extremely high extinction coefficients (typically $10^6 - 10^7 \text{ M}^{-1}\text{cm}^{-1}$), and high quantum yield (up to 80%). The amplified fluorescence responses arise from delocalization of π^* excited states which allows excitons to easily diffuse through a polymer chain.⁴⁴

Table 1. Commercial products of fluorescent polymer NPs.

Company	Brand	Fluorescence Ex _{max} /Em _{max} (nm)	Sizes (μm)	Functional groups
Thermal Fisher	Fluoro-Max	Green(468/508)	0.03-10	
		Red (542/612)	0.03-3	
		Blue (365/447, 412/447, 412/473)	0.05-2	
Invitrogen (Molecular Probes®)	FluoSpheres®	Blue (350/440, 365/415)	0.02, 0.2, 1, 2	Carboxyl
		Yellow-green (505/515)	0.02, 0.04, 0.1, 0.2, 0.5, 1, 2	
		Nile Red(535/575)	0.02, 1, 2	
		Orange (540/560)	0.04, 0.1, 0.2, 1	
		Red-Orange (565/580)	0.04	
		Red (580/605)	0.02, 0.04, 0.1, 0.2, 0.5, 1, 2	
		Crimson (625/645)	0.02, 0.2, 1	
		Dark Red (660/680)	0.02, 0.04, 0.2	
		Infrared(715/755)	0.04, 0.1	
		Blue(365/415)	1, 4	Sulfate
		Yellow-Green (505/515)	0.02, 0.2, 1, 2, 4	
		Red (580/605)	1, 4	
		Yellow-Green (505/515)	0.01, 1	Aldehyde-Sulfate
		Yellow-Green (505/515)	0.02, 1	Amine
		Red (580/605)	0.02	
	SAIVI™ 715 injectable contrast agent	715/775	0.1, 2	
Polysciences	Fluoresbrite® carboxylated microsphere Latex Beads	Blue (360/407)	0.05,0.1,0.5,1,1.75,4.5,6,10	Carboxyl
		Yellow Green(441/468)	0.1,0.2,0.3,0.35,0.4, 0.5,0.75,1, 1.75, 2, 3, 4.5, 6, 10	
Sigma-Aldrich		Yellow Orange (529/546)	0.1, 0.2, 0.5, 1, 1.75, 3, 4, 5, 6	
		Blue (360/420)	0.05, 2	Amine
		Yellow-green (470/505)	1	
		Red (575/610)	1	
		Orange (481/644)	0.1, 1, 2	
		Yellow-green (470/505)	0.03, 1, 2	Carboxyl
		Red (575/610)	0.05, 1	
		Orange (481/644)	0.5, 2	
		Blue (360/420)	0.1, 0.5, 1, 2	Sulfate
		Yellow-green (470/505)	0.1	
		Red (575/610)	0.03, 0.05, 0.1	

In one example of polymer NPs used in stem cell tracking, Fluosphere® conjugated to Nile Red was used to assess the recruitment, and vasculogenesis, that is, homing and vascular channel formation by circulating stem/progenitor cells (SPCs) in subcutaneous Matrigel, an endothelial cell basement membrane-like material that is a liquid at 0°C and a solid at body temperature,⁴⁵ supplemented with lactate polymer in mice.⁴⁶ Matrigel plugs were injected subcu-

taneously into the back of mice on either side of the thoracic vertebrae. The presence of functional vascular channels in the Matrigel was documented by injecting mice with 40nm carboxylate-modified Fluosphere® (Invitrogen) conjugated to Nile red. Results showed that SPCs were among the earliest cells to arrive at a subcutaneous Matrigel target and were recruited to Matrigel in a large cell number.⁴⁶ (Figure 1).

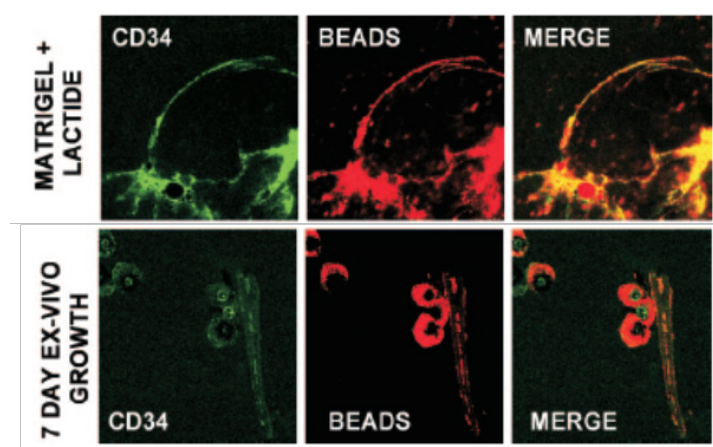


Fig 1. Matrigel implants were thinly sliced, and cells were labeled with specific anti-mouse CD34-FITC in 1:100 dilutions for 60 min on ice and then placed onto a glass slide for observation. CD34 is the surface marker of SPC. The presence of functional vascular channels in the Matrigel was documented by injecting mice with 40nm carboxylate-modified FluoSpheres® conjugated to Nile red. Top row is SPC surface marker CD34 expression and vascular channels identified by Nile red beads in Matrigel harvested 18 h post implantation. The bottom row shows images of Matrigel incubated ex vivo for 7 days. Note that each row shows images from different samples. Even at just 18 h after implantation, channels could be visualized. CD34 cells lined these channels, indicating vasculogenesis of SPCs in Matrigel. (Reprinted and adapted with permission from ASM, reference 46.)

However, the reports of using fluorescent polymer NPs in direct labeling and tracking stem cells are few. Fluosphere® and Fluoresbrite® are the more frequently used in phagocytosis assessment of phagocytic cells, such as dendritic cells,^{47, 48} monocytes,⁵¹ neutrophils,⁵⁰ macrophages,⁵¹ differentiated from stem cells from different origins.

3.2. Quantum Dots

Quantum dots (QDs) are colloidal, crystalline semiconductor NPs made from II-VI or III-V elements (e.g. PdS, CdSe).²³ Their electronic and optical characteristics are closely related to the size and shape of the individual crystals. In general, smaller sized QDs have shorter emission wavelength.⁵² QDs have unique absorption and emission properties that differentiate them from conventional fluorescent dye molecules. Specifically, QDs have broad absorption range from ultraviolet (UV) to visible, but exhibit distinct emission spectrum with narrow full width at half maximum (FWHM) (typically 10-40nm).⁵³ QDs are more resistant (can be up to 100 times) to photochemical degradation than fluorescent dyes, which

makes them useful for tracking cells and monitoring biological changes over extended periods of time.⁵⁴ Despite many advantages, QDs have inherent problems. QDs generally contain heavy metal ions such as Cd²⁺, Pd²⁺, Se²⁺, which are toxic.⁶⁰ Stochastic blinking has also been observed for QDs. The involvement of dark states and blinking phenomena in QDs requires higher doses in order to yield the desired brightness and to increase the accuracy of quantitative measurements in cell tracking, cell imaging or other biological applications.⁵⁵ However, higher doses may decrease signal to noise ratio and increase non-specific binding.

Currently, QDs are distributed by many large companies like Invitrogen, Millipore, eBioscience, Thermo Fisher, Sigma-Aldrich, Millipore, and Nanoco Technologies. Small vendors exist as well including Ocean Nanotech, Crystalplex, Nanoaxis *etc.* Amongst the numerous QD products, Qdot® (Invitrogen) is most frequently used for stem cell labeling and tracking, seconded by efluor® (eBioscience). Nanoco Technologies claims it is the only supplier of heavy metal-free quantum dots CFQD™ (cadmium-free

quantum dots) which show bright emission from UV through the visible spectrum, and into the near infra-red.⁵⁶ All existing QDs products are expensive (\$150-\$300 per micro molar). Thus it is necessary to improve the reaction methods to significantly reduce the cost of QDs and develop green chemistry to produce non-toxic QDs in order to satisfy the growing market need. Table 2 summarizes existing QD products from several major distributors.

Many have reported tracking of QDs labeled stem cells *in vitro* and *in vivo*. For example, Slotkin *et al* developed an ultrasound-guided *in vivo* delivery technique to efficiently label neural stem and progenitor cells (NSPCS) of the developing mammalian cen-

tral nervous system with COOH-conjugated Qdot[®] 620.⁵⁷ In their study, COOH-conjugated Qdot[®] 620 were injected into the parenchyma of the caudal ganglionic eminence (CGE) of the ventral telencephalon of E13.5 mouse embryos (Figure 2A). After 5 days, Qdot[®]s were found in each of the three principle cell types differentiated by NSPCS, including GFAP+ astrocytes, NG2+ oligodendrocyte progenitors and β III tubulin+ neurons (Figure 2B-D). Those three principle types of cells were found substantial distances away from the initial site of injection, which indicated that Qdot[®] labeled NSPCS *in vivo* differentiated and migrated during the period studied.

Table 2. Commercial products of QDs from major distributors.

Company	Brand	Emission (nm)	Functional groups	Available conjugates
Invitrogen	Qdot [®]	525, 545, 565, 585, 605, 655, 705, 800	Amine, Carboxyl, ITK [™] organic	Primary antibody, secondary, antibody, Avidin, Streptavidin, Biotin, Lectin, Isotype control
eBioscience	eFluor [®] Nanocrystal	490, 525, 545, 565, 585, 605, 625, 650, 700	Amine, Carboxyl	Primary antibody, secondary, antibody, Streptavidin, Isotype control
Millipore	Quantum Dot	525, 565, 605, 655	N/A	Secondary antibody, Streptavidin
Sigma-Aldrich	Lumidot [™] CdS	380, 400, 420, 440, 460, 480	N/A	N/A
	Lumidot [™] CdSe	480, 520, 560, 590, 610, 640	N/A	N/A
	NanoGreen [™] CdSe/ZnS QDs	485, 530, 590, 610, 635		
	Trilite [™] CdSeS/ZnS alloyed QDs	490, 525, 540, 575, 630, 665	Carboxyl	
Nanoco Technologies	NanoDot [™] (CdSe/ZnS)	480, 510, 530, 560, 590, 610, 640		
	CFQD [™] (Cadmium free)	400 to 650	Hexadecylamine (HDA)	N/A
	CdSe QD Cores	480, 520, 560, 590, 610, 640	HDA or HDA/Trioctylphosphine oxide(TOPO)	N/A
	CdS QD Cores	370-390, 390-410, 410-430, 430-450, 450-470, 470-490	Carboxyl	N/A
Ocean nanotech	Water soluble quantum dots	450, 490, 525, 540, 580, 600, 620, 645, 665	Monolayer of oleic acid/octadecylamine with a monolayer of amphiphilic polymer, PEG, polydiallyldimethylammonium chloride (PDDA), phenylboronic acid (PBA).	N/A
	Water soluble heavy metal free QD	530, 580, 655	Amphiphilic polymer with terminal carboxyl groups	
Crystalplex	Trilite [™]	490, 525, 575, 630, 665	Carboxylamine, Hydroxyl, Alkyl	N/A
Nanoaxis	AxiCad [™]	530, 560, 590, 630, 680, 740	Mercapto acid/Cysteine	Antibodies, peptides

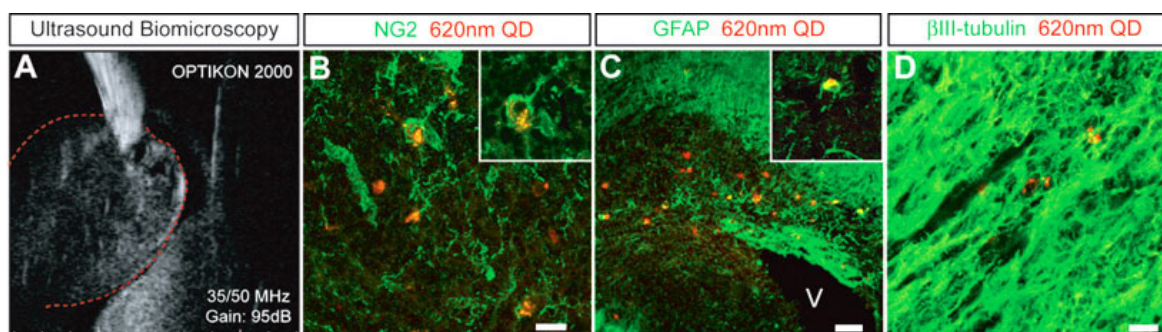


Fig 2. Qdot® forneural stem and progenitor cells (NSPC) tracking in the developing mammalian central nervous system. **A:** Qdot® 620 were injected into the caudal ganglionic eminence of embryonic E13.5 mouse brains with the aid of high-resolution ultrasound biomicroscopy. **B–D:** In a coronal view of E18.5 developing cerebral cortex, intracellular labeling by Qdot® 620 was observed in NG2+oligodendrocytes (B), GFAP+ astrocytes (C), and β III-tubulin+ neurons (D). (Reprinted and adapted with permission from John Wiley and Sons, reference 57).

Table 3. Fluorescent silica NPs from HST and Microsphere-Nanosphere.

Company	Brand	Fluorescence Exmax/Emmax (nm)	Available size (μ m)	Functional groups
Hybrid Silica Technologies	C•spec®	FITC, Rhodamine Green (488/517) ATTO488(501/523) TRITC (550/570) Texas Red(596/617) Cy5 (650/670) Cy5.5 (675/694) ATTO647N, ATTO647 (644/669)	0.01, 0.025, 0.045, 0.075, 0.1, 0.5	NHS ester, Carboxyl, amine, Maleimide, streptavidin, PEG, PEI, Cyclic RGD, TAT peptide
Microsphere-Nanosphere	Blue (354/450)		0.05, 0.2, 0.5, 1, 1.5, 4	non-modified
	Green (485/510)		0.02, 0.03, 0.05, 0.1, 0.2, 0.3, 0.4, 0.5, 0.6, 0.7, 0.8, 0.9	non-modified
			0.05, 0.2, 0.3, 0.5	Amine, Carboxyl
	Red (569/585,)		0.05, 0.2, 0.3, 0.5, 1, 1.5, 3, 4, 5, 10	non modified or Amine

3.3 Fluorescent silica NPs

Besides fluorescent polymer NPs and QDs, another type of fluorescent NP is silica NP containing organic dye molecules. In this system, silica acts as matrix to chemically and mechanically stabilize the fluorescent dyes. The silica partially protects the dye molecules from external quenchers, enhances the photostability of incorporated dyes, and in some cases, provides a biocompatible and easy-to-functionalize surface for bioconjugation.²⁴ Fluorescent silica NPs are mainly made through two approaches: sol-gel or reverse microemulsion. Sol-gel method usually generates fluorescent silica NPs in the hundreds of nanometers to micron range,⁵⁸ while reverse micro-emulsion strategy provides NPs with diameters from nano to micro size.^{60, 61, 62} And in both methods, the spectral character of silica NPs is determined by the dye molecules encapsulated.

In comparison to many vendors of fluorescent polymer NPs and QDs, fluorescent silica NPs are mainly provided by two companies, namely Hybrid

Silica Technologies (HST) and Microsphere-Nanosphere Inc. C•spec® NPs from HST have a “core-shell” structure with dye rich core and silica shell (Figure 3). The synthesis of C•spec® involves two processes.⁶³ First organic dye molecules are covalently attached to a silica precursor to form adduct of the dye-rich core materials.⁶³ Second, silica sol-gel monomers are subsequently co-condensed with the core in specific order depending on the desired architecture to form a denser silica shell around the core.⁶³ The size of C•spec® can be precisely controlled, ranging from 4nm to 100nm by varying the thickness of silica shell. The silica shell provides shielding of dye molecules from solvent interactions which can be detrimental to their photostability.⁶³ Further, this core-shell approach provides versatility of placement of the dye molecules within the silica nanoparticles, such as placing the dye molecules in an intermediate layer of the particle surface.⁶³ Those small changes in the internal architecture of particles with otherwise similar composition can alter the radiative rate and nonradiative rate of the dye which vary inversely

with the degree of rotational mobility of the dye allowed by the particle architecture. Thus the enhancement of quantum yield of fluorophores can be selectively modified by manipulating the internal particle architecture.⁶⁴ Due to aforementioned increase of quantum yield of dye molecules result from the unique core-shell structure as well as encapsulation of multiple dye molecules into a single particle,⁶⁶ C•spec[®] are significantly brighter and more stable than free dyes in aqueous solutions.⁶⁵ For example, 30 nm C•spec[®] Tetramethylrhodamine (TRITC) NPs have a brightness as 30 fold as that of the precursor (i.e. TRITC) and approach that of same sized quantum dots (Figure 4).⁶⁵

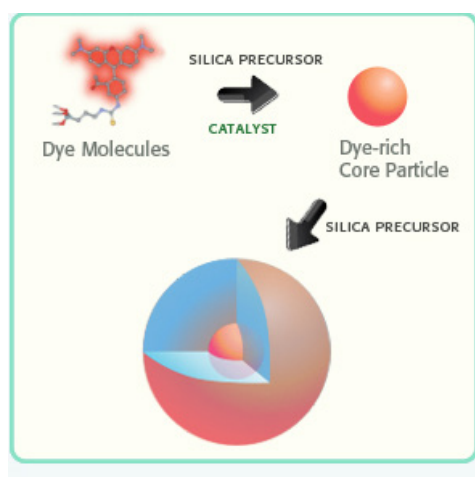


Fig 3. Schematic illustration of the synthesis of a C•spec[®] NP: the organic dye molecules are covalently bound into a silica-based core. Then the core is grown into a core-shell NP (Reprinted and adapted with Permission from HST, Reference 65).

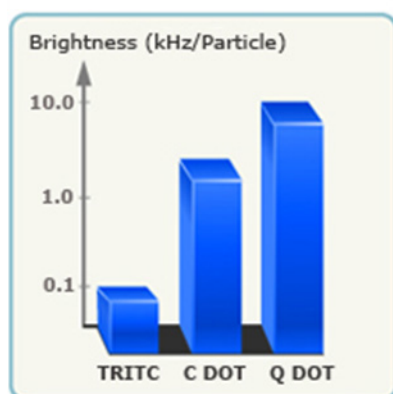


Fig 4. Brightness measurements (log scale) of C•spec[®] NPs relative to constituent dye (TRITC) showing the brightness enhancement, as well as a comparison to QDs of similar size and wavelength. (Reprinted and adapted with permission from HST, Reference 65).

Compared with fluorescent polymer NPs and QDs, fluorescent silica NPs are advantageous in terms of their surface functionalities and biocompatibility. Commercial fluorescent polymer NPs are usually available with carboxylic acid, sulfate, aldehyde, and amine surface functionalities. C•spec[®] includes broader selections of surface functionalities, such as NHS ester, carboxyl, amine, sulfhydryl, maleimide, streptavidin, polyethylene glycol (PEG), polyethylenimine (PEI), cyclic arginylglycylaspartic acid (RGD), transactivator of transcription (TAT) peptide, primary antibody and secondary antibody. Furthermore, fluorescent silica NPs are presently the only type of fluorescent NP approved for human clinical trials. In January 2011, 7nm Cy5 encapsulated fluorescent silica NP was approved for Investigational New Drug Application (IND) from the US Food and Drug Administration (FDA) as an ultra small silica inorganic NP platform for targeted molecular imaging of cancer. Considering the growing demand from the field of stem cell labeling and tracking in clinical trials (940 clinical trials involving stem cells are funded by U.S national institute of health from 2002 to 2007. The number of funded stem cell clinical trials increased almost three fold to 2780 cases from 2007 to 2012),¹¹⁶ silica-based fluorescent NPs like C•spec[®] have great potential to help advance our understanding and management of stem cell based research and therapy.

So far, there is no report applying fluorescent silica NPs for stem cell labeling and tracking. However, fluorescent silica NPs produced in research laboratories were referred extensively in publications of cell labeling and tracking. For example, cyanine dye-doped silica NPs were reported to directly discriminate live and early-stage apoptotic stem cells (both mesenchymal and embryonic) through a distinct external cell surface distribution,⁶⁸ which makes them ideal for stem cell labeling and tracking.⁶⁷ Recently, Cy5 encapsulated 7nm fluorescent silica NPs were functionalized with both cyclic RGD peptide and radioactive iodine for tumor imaging in a mouse model of melanoma.⁶⁹ (Figure 5A) This ultra-small multimodal silica NPs exhibited high-affinity binding, favorable tumor-to-blood residence time ratios, and excellent tumor-selectivity on $\alpha_v\beta_3$ integrin-expressing melanoma xenografts in mice. The tumor sites accumulated with fluorescent silica NPs were visualized with both PET (Figure 5B&C) and fluorescent imaging (Figure 5D&E).⁶⁹

4. Magnetic NPs for stem cell labeling and tracking with MRI

Magnetic NPs could be categorized as T1 or T2

contrast agents for MRI depending on the relaxation processes. T2 contrast agents include superparamagnetic iron oxide NPs (SPION), bimetallic ferrite NPs (e.g. CoFe_2O_4 , MnFe_2O_4 , and NiFe_2O_4), and hybrid magnetic NPs such as Fe_3O_4 -Au dumbbell NPs.⁷⁰ So far, SPIONs are the only commercial NPs that have been regulated for clinical applications.⁷³ Other types of magnetic NPs are still in the experimental stages and only produced at the lab scale. T1 contrast agents are primarily gadolinium (Gd) containing NPs (e.g. Gd-chelated lipid NPs, Gd-chelated dextran NPs) and gadolinium oxide NPs.⁷⁰ Considering the stability, biocompatibility, and accessibility, SPIONs and gadolinium oxide NP are the most popular choices for T2 and T1 MRI based stem cell labeling and tracking respectively.

4.1. Superparamagnetic iron oxide NPs (SPIONs)

SPIONs comprise of an iron oxide core, which is mostly magnetite Fe_3O_4 or maghemite $\gamma\text{-Fe}_2\text{O}_3$, a coating layer, and surface functional groups.³ The coating and surface functional groups provide hy-

drophilicity, stability, and functionality.³ SPIONs can be prepared by the co-precipitation method, in which metal ions (e.g. Fe^{2+} and Fe^{3+}) are co-hydrolyzed in a basic solution ($\text{NH}_3\cdot\text{H}_2\text{O}$) under the presence of surfactants (e.g. dextran).^{3, 74} They can also be prepared through high-temperature decomposition of metal precursors (e.g. $\text{Fe}(\text{CO})_5$) in organic solvents (e.g. octyl ether) under the presence of surfactants (e.g. oleic acid), which provides better control over the size and crystallinity than the co-precipitation method.^{3,75}

Guerbet, AMAG Pharmaceuticals and Bayer Schering Pharma AG are the major players in this field. Besides those big pharmaceutical companies, many chemical companies also supply SPION products with different size ranges, coatings and surface functionalities. Table 4 includes a list of existing SPION NP products. The products listed in upper part of Table 4 are supplied by pharmaceutical companies, and are FDA approved or under clinical trials. The products listed in the bottom part of Table 4 are SPION products from chemical suppliers.

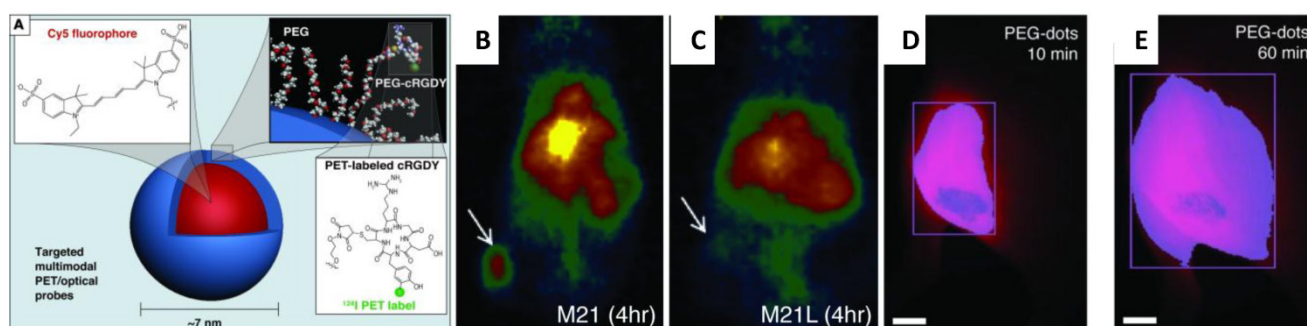


Fig 5. (A) Schematic illustration of the 124I-cRGDY-PEG-ylated core-shell silica NP with surface-bearing radiolabels and peptides and core-containing reactive dye molecules (insets). (B) Representative whole-body coronal micro PET images at 24-hours demonstrating M21 (left, arrow) tumor uptakes of 3.6 %ID/g. %ID/g indicates the percentage of the injected dose (ID) of PEG-silica NP per gram tissue. (C) Enhanced M21 tumor contrast at 24 hours (right). (D) Whole-body fluorescence image of the tumor site 10 minutes after subdermal PEG-silica nanoparticle injection. (E) Delayed whole-body fluorescence image of the tumor site 1 hour after PEG-silica NP injection. (Reprinted and Adapted with permission from ASCI, reference 69).

Table 4. Commercial SPION.

Company	Brand ^b	Size (nm) ^a	Coating
I) SPION approved by FDA or under clinical trials from pharmaceutical companies			
Guerbet, AMAG Pharm, Inc	Ferumoxides ^d	120-180	Dextran T10
	AMI-25		
	Feridex/Endorem		
	Ferumoxtran-10	15-30	Dextran T10, T1
	AMI-227		
	Combix/Sinerem		
Bayer Schering Pharma AG	Ferucarbotran	60	Carboxydextran
	SHU 555A		
	Resovist		
	SHU 555C	21	carboxydextran
	Supravist		

	Ferumoxytol Code 7228	30	Polyglucose sorbitol carboxymethyl ether
GE-healthcare	Feruglose NC-100150 Clariscan	20	Pegylated Starch
Ferropharm	VSOP-C184	7	Citrate
II) SPIO products from different chemical companies			
Sigma-Aldrich	Superparamagnetic iron oxide nanoparticles	5nm, 10nm ^c	1.0% modified short chain polyethylene glycol (PEG)
Oceannanotech	IDX	5-10	Dextran
	ILP	10, 20, 30	lipid
	ILA	10, 20, 30	Lipid with terminal amine groups
	SMG	10, 20, 30	Amphiphilic polymer, PEG
	SHQ	10	Amphiphilic polymer, polydiallyldimethylammonium chloride (PDDA)
	SEI	10, 15, 20, 25, 30	Amphiphilic polymer, polyethylenimine (PEI)
	SHP	5, 10, 15, 20, 25, 30	Amphiphilic polymer with carboxylic acid groups
	SHA	10, 15, 20, 25, 30	Amphiphilic polymer with amine groups, PEG
	SXP	5, 10, 15, 20, 25, 30, 40	Amphiphilic polymer with carboxylic acid groups, endotoxin free
Nanocomposix	Magnetite nanoparticle	5.4nm	Tetramethyl amine
NN-Labs, LLC	Magnetic iron oxide nanocrystals in water	5, 10, 20	
TurboBeads	TurboBeads Amine	30	Primary aliphatic amine groups
	Turbobeads Carboxyl	30	Carboxyl groups
Sciventions	Magnetite	1-10	Polyacrylate sodium
Chemicell	fluidMAG-ARA	50,75, 100, 150, 200	Glucuronic Acid
	fluidMAG-Chitosan	50,75, 100, 150, 200	Chitosan
	fluidMAG-CMX	50,75, 100, 150, 200	Carboxylmethyl dextran
	fluidMAG-D	50,75, 100, 150, 200	Starch
	fluidMAG-DEAE	50,75, 100, 150, 200	DEAE-starch
	fluidMAG-DX	50,75, 100, 150, 200	Dextran
	fluidMAG-DXS	50,75, 100, 150, 200	Dextran-sulfate
BioPAL	Molday ION™	35	Rhodamine, C6amine,

a. Hydrodynamic size. b. all used brandnames of the same compound are listed. c. TEM size. d. Feridex® was discontinued by Guerbet, AMAG Pharm, Inc in 2009 because it competed with other MRI contrast agents sold by Guerbet, AMAG Pharm, Inc.

SPIOs have been used as MRI contrast agents since 1990.⁷² Currently, they are clinically used for liver imaging,^{70, 72} lymph nodes imaging,⁷⁰ and blood pool agent.⁷⁰ Although not initially developed for stem cell labeling and tracking,⁷⁰⁻⁷⁸ they have been successfully adapted for tracking stem cells post implantation.^{78, 79} Among them, Ferumoxides and ferucarbotran are most frequently used probably because of the regulation by U.S. Food and Drug Administration (FDA) and European Medicines Agency (EMA). Since the approval by FDA in 2009 for iron-deficiency anemia, ferumoxytol also attracts lots of attention as contrast agents for stem cells tracking.⁷⁷ All three NPs have been successfully used to label rat or human mesenchymal stem cells (MSCs),^{80, 82} embryonic stem cells (ESCs),^{84, 86} olfactory ensheathing cells (OECs),⁸¹ and neural stem cells (NSCs)^{83, 84}. For example, NSCs

harvested from brain tissue of neonatal Sprague Dawley rats were labeled with ferucarbotran (Resovist®) and transplanted into rats of middle cerebral artery occlusion model by injection of cell suspension into ventricles.⁸⁰⁻⁸⁷ Following injection, MRI revealed that NSCs migrated from right lateral ventricle to the cerebral ischemic regions 2 weeks post-transplantation (Figure 6).⁸⁷

The number of publications using SPIO in stem cell labeling or tracking increased exponentially in recent years (Figure 7). The majority of those studies are conducted in North America, Europe and East Asia. The significant increase of the number of publications indicates the great potentials of SPIOs and a rising “market share” in the field of stem cell labeling and tracking. However, stem cell labeling using SPIOs is presently not a FDA approved indication because

how SPIOs affect the function and fate of stem cells is not clearly understood.⁸⁸

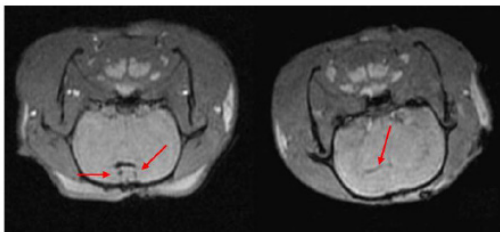


Fig 6. MRI of transplanted Resovist[®]-labeled NSCs in the rat brain. At 1 hour following transplantation of Resovist[®]-labeled NSCs (T2 fast-gradient echo sequence), arrows reveal two symmetrical and horizontal pinholes (left). At 2 weeks post-transplantation, the arrow reveals the migration of Resovist[®]-labeled NSCs from the right lateral ventricle to the ischemic area (right). (Reprinted and adapted with permission from NRR, reference 87).

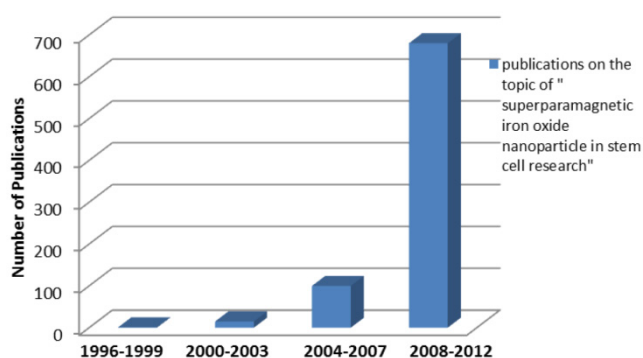


Fig 7. Survey of publications related to “superparamagnetic iron oxide nanoparticle in stem cell research” in the Web of Science database as a function of publication years (3 years as a data point) for the indicated combination of words in the title and/or abstract. The number of publications shows the rapid increasing interest in stem cell and particle tracking in the literature. In other words, the trend of increasing number of publications indicates a rising “market share” of superparamagnetic iron oxide in stem cell related research.

4.2 Gadolinium oxide NPs

Different from T2 agents that produce negative signal (dark spots) on MRI images, Gadolinium based T1 agents produce bright positive signal. As they are bigger compared with conventional Gadolinium chelates, gadolinium oxide NPs should permit higher cell uptake and longer retention in labeled cells.⁸⁹ Currently, the use of gadolinium oxide NPs in cell tracking is still at early stage due to the insufficient understanding of their stability in cells and their cytotoxicity on cell functionality.³ GadoCellTrack[™] is the only commercial gadolinium oxide NP in the market. Developed by BioPAL Inc, GadoCellTrack[™] is a negatively charged 50nm Gd₂O₃ NP for tracking cells *in vivo* by MRI. According to BioPAL, this reagent provides a strong T1 signal that is comparable to the same

molar concentration as Gd-DTPA.⁹⁰ GadoCellTrack[™] has been used to label human aortic endothelial cells and the T1 enhancement of the internalized NP maintained for up to 7 days.^{91,92} We must notice that cell viability and proliferation could be affected with GadoCellTrack[™] labeling. Prior to apply gadolinium NPs in stem cell therapy, their effects on stem cell function needs to be fully investigated.

5. Commercial NPs for photoacoustic imaging

Gold (Au) NPs, Au nanorod, and single walled carbon nanotubes (SWNTs) are potential contrast agents for photoacoustic imaging.^{93,94} Concerning the safety issue, SWNTs have not been utilized for stem cell labeling and tracking. Au NPs and Au nanorods are currently the popular choices because of their tunable optical properties and excellent biocompatibility.^{27,95-97}

Currently, Au NPs and Au nanorods can be purchased from Sigma-Aldrich, Strem Chemicals and Ted Pella as well as small companies specialized in NP products like Nanopartz, ocean nanotech, and nanocomposix *etc* (Table 5). Among those products, Accurate[™] (Nanopartz), NanoXact[™] (Nanocomposix), Biopure[™] (Nanocomposix) and water soluble Au NPs (Ocean nanotech) are available from sub-10 to 125nm with peak surface Plasmon Resonance (SRP) from 515 to 572nm. Au nanorods are available with diameter ranging from 10 to 50 nm with aspect ratio from 1.9 to 17.9, whose peak SRP covers from visible to near infrared. Nanopartz provides Au nanorods with the largest selection of axial diameter, aspect ratio and peak SPR amongst all distributors. Ntracker[™] and Ntherapy[™] from Nanopartz are specifically developed for use in *in vivo* imaging.

Photoacoustic imaging provides high detection sensitivity, which allowed imaging of down to 100,000 cells *in vivo* and high spatial and temporal resolution which are at least an order of magnitude below traditional cell imaging techniques, such as positron emission tomography (PET).⁹⁸ Because of its low-cost, deep penetration (up to 2cm), non-invasiveness, and good resolution (100μm), photoacoustic imaging is becoming an alternative method of fluorescent imaging, MRI and radioactive imaging for stem cell labeling and *in vivo* tracking.^{27,96,98} In a recent study, MSCs were pre-labeled with Au NPs before their incorporation into PEGylated fibrin gel (Figure 8).²⁷ Then fibrin gel was injected intramuscularly in the lateral gastrocnemius of an anesthetized Lewis rat. The contrast brought by Au NPs allowed the researchers to visualize the *in vivo* differentiation and neovascularization of MSCs using photoacoustic imaging.²⁷

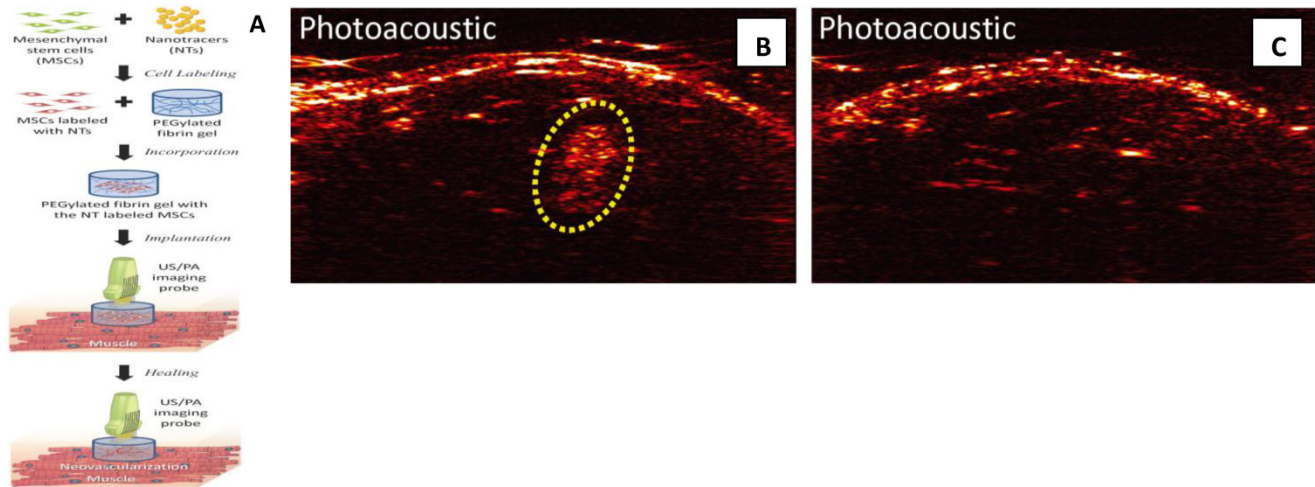


Fig 8. MSCs tracking with photoacoustic imaging: (A) Once MSCs are loaded with Au NPs, the labeled MSCs are entrapped in the PEGylated fibrin gels and implanted at the ischemic region. The PEGylated fibrin gels promote MSC differentiation toward a vascular cell type, thus contributing to regeneration. Both MSC distribution and neovascularization can be monitored using the combined ultrasound and photoacoustic imaging of cells loaded with Au NPs. (B,C) *In vivo* monitoring of Au NP labeled MSCs using photoacoustic imaging. (B) *In vivo* Photoacoustic images of the lateral gastrocnemius (LGAS) of an anesthetized Lewis rat in which PEGylated fibrin gel containing Au NT loaded MSCs was injected. PEGylated fibrin gel location is outlined with yellow dotted circle. Injection depth was about 5 mm under the skin. (C) Control at the region of the LGAS of the other hind limb without any injection. Photoacoustic images were acquired at the wavelength of 760 nm with a fluence of 11 mJ/cm². (Reprinted and adapted with permission from PLOS, reference 27).

Table 5. Commercial Au NPs and Au nanorods.

Company	Product name	Size diameter (nm)	Peak SPR wave (nm)	Coating/stabilizer
Sigma-Aldrich	Gold nanoparticle	5, 10,	515-520	citrate
		20,	524	
		30,	526	
		40,	530	
		50,	535	
		60,	540	
		80,	553	
Sigma-Aldrich	Gold nanorod	10X38	780	Cetrimonium bromide (CTAB)
		10X41	808	
		10X45	850	
		10X59	980	
Nanopartz	Ntracker™	10X38	780	Hydrophilic polymer terminated with methyl group
		10X41	808	
		10X45	850	
		10X59	980	
		10X67	1064	
	Ntherapy™	10X38	780	Hydrophilic polymer terminated with amine or carboxyl, As33scFv, Chitosan, anti-EGFR,DNA Oligos, Glutathione, Folate, CD33, CD24, CD45,EPCAM, Doxorubicin,T-Cells, anti-CD4, polyethylenimine proprietary carboxylic acid, citrate, Amine, biotin, Maleimide, methyl, Neutravidin, NHS, streptavidin, Azide, MUTAB, secondary antibodies, protein A
		10X41	808	
		10X45	850	
		10X59	980	
		10X67	1064	
Nanopartz	Accurate™ Spherical Gold Nanoparticles	1.8, 2.2, 3, 4, 5, 10, 15, 20, 25, 30, 35, 40, 45, 50, 55, 60, 65, 70, 75, 80, 85, 90, 95,100, 125		
		Gold Nanorodz™	10X 67, 59, 50, 45, 41, 38, 35,29	1064, 980, 900, 850, 808, 780, 750, 700

			980, 850, 808, 780, 750, 700, 650, 600, 550, 60, 47, 34,	Neutravidin, NHS, streptavidin, MUTAB, secondary antibodies
			750, 700, 650, 600, 550, 700	
		40X	138, 118, 97, 76, 55,	
		50X	147	
Strem chemical, Inc	Gold nanoparticle	5	515-520	Surfactant free, citrate, CTAB,
		10	520	
		15	520	
		20	524	
		30	526	
		40	530	
	Gold nanorod	10X	29	700
		10X	35	750
		10X	38	780
		10X	41	808
		25X	34	550
		25X	47	600
		25X	60	650
		25X	73	700
Nanocomposix	Nano Xact™	5, 7, 10,	520	Tannic acid, citrate, Polyvinylpyrrolidone (PVP)
		12, 15, 17, 20, 30, 40,		
		50, 60, 70, 80, 90, 100	525, 530, 535, 545, 555	
			555	
	Biopure™	5, 7, 10, 12, 15, 20, 30, 40	520	Tannic acid, PVP
		50, 60, 70, 80, 90, 100	525, 530, 535, 545, 555	
			555	
Ted Pella,	PELCO®	5, 7, 10, 12, 15, 17, 20, 30, 40	520	Tannic acid
	Nano Xact™	50	525	
		60	530	
		70	535	
		80	545	
		90	555	
		100	555	
	PELCO®	5, 7, 10, 12, 15, 17, 20, 30, 40	520	Tannic acid
	Biopure™	50	525	
		60	530	
		70	535	
		80	545	
		90	555	
		100	555	
Nanocomposix	Biopure™ Gold colloids coated with silica shell	17	525	10-20nm silica shell non functionalized or amine terminated
		30	528	
Ted Pella	PELCO®	50	533	
	Biopure™ Gold colloids coated with silica shell			
Oceannanotech	UEI			PEI
	AUA			Amphiphilic polymer terminal with Amine /PEG
	AUH	6	520	Amphiphilic polymer with terminal carboxylic acid groups
	LyoF™			Carboxylic acid
	AclaF™	15, 20, 25, 30, 35, 40, 45, 50,	520, 520, 528, 527, 523, 527,	Amphiphilic polymer with carboxylic acid groups
		60, 70, 80, 90, 100	538, 528, 537, 542, 546, 550, 563	

	GNP		Un-coated
	GRN	10X34, 10X39, 10X43, 10X51, 20X51, 20X66 20X75, 20X84, 20X95, 40X68, 40X84, 40X96	
NN-Labs	Au Dot nanocrystal	5, 10, 20	citrate

6. Concerns and perspectives

So far, we have summarized the existing commercial NPs which could act as contrast agents of three commonly used modalities (namely fluorescent imaging, MRI and photoacoustic imaging) for labeling and tracking of stem cells. Amongst them, SPIOs as MRI contrast agents have the longest history of commercialization and use in cell labeling and *in vivo* tracking. Commercial fluorescent NPs, such as QDs, fluorescent polymer NPs and fluorescent silica NPs, have undergone an exciting development in the past decade. In particular, the commercialization of QDs was a huge success. Research of using QDs in stem cell therapy is extensively investigated. However, the cytotoxicity of QDs is still controversial. Fluorescent silica NPs can be a biocompatible alternative of quantum dots. Products of Au NPs and Au nanorods have been commercialized for many years, although their application in labeling and tracking stem cell is recently found. With the rapid development of nanotechnology in stem cell therapy, the list of commercial NP products will quickly expand.

Despite these successes and great potentials, concerns exist for these commercial NPs, including cytotoxicity, signal loss in longitudinal tracking during stem cell division and proliferation, insufficiency of single modality NPs to attain comprehensive information of cells post transplantation, and limited capability to report cell functionality and viability. It is critical to address these questions before they are formally used in clinic treatments.

6.1 Safety profile of commercial NPs

No NP has been approved by FDA for the purpose of labeling and tracking stem cells in the therapy as of yet. Prior to their usage in the clinics, it is necessary to fully characterize their effects on stem cells (i.e. cytotoxicity), including the viability, differentiation, migration/homing, distribution, and engraftment. It is challenge because the cytotoxicity of NPs depends on many parameters such as NP composition, shape, size, concentration, and surface functional groups.⁹⁹ For example, the most intensively studied SPIOs are generally considered as non-toxic,⁹⁹ but poly-L-lysine labeled SPIOs could impair the osteogenic and chondrogenic differentiation potentials of MSCs.¹⁰⁰ Due to the complexity of the subject matter, sometimes, re-

ports are contradictory to each other.^{89,100} Ramaswamy *etc* reported successful labeling MSCs using Feridex[®] without impair cell chondrogenesis differentiation,¹⁰¹ while Bulte *etc* reported that chondrogenic differentiation of MSCs is inhibited after labeling with Feridex[®].¹⁰² Therefore, during our investigation, we should be careful, cautious, and sensitive to other's reports.

6.2 Signal loss in longitudinal tracking

Longitudinal tracking is important to study the efficiency of stem cell therapy and stem cell engraftment level. One issue of using NP for long term stem cell tracking is the signal loss resulted from cell division and exocytosis,^{3, 104, 105} which limits the application of NPs in stem cell therapy. One possible solution is to develop new products with strong signal which provide detectable signal after multiple cell divisions. Single particle detection in single cell should open up new possibilities for cellular imaging and guide the development of new products.^{33, 106} In the case of single particle single cell detection, after multiple cell divisions one stem cell contains only one single particle whose signal should still be sufficient for detection. Xu *etc* demonstrated the possibility of single particle single cell detection for stem cell therapy. Biodegradable poly(lactide-co-glycolide) microparticles encapsulating multiple 10nm iron oxide NPs (Iron oxide/PLGA-Micro particles, 0.4–3 μ m) in MSCs enhances MR parameters such as the R2 relaxivity (5-fold), residence time inside the cells (3-fold) and R2 signal (2-fold) compared to 10nm iron oxide NPs alone.²⁵ MRI signal is still detectable in MSCs labeled with iron oxide/PLGA-Micro particles up to 12 days, while minimal signal can be detected in MSCs labeled with 10nm iron oxide NPs.³³ Micro-complex encapsulating multiple copies of SPIOs may become a new type of product of MRI contrast agent which provides high resistance to signal dilution and would advance the use of NP for long term tracking of stem cells.

6.3 Limitation of single modality NPs

No existing single modality is sufficient to attain all necessary information of transplanted cells.¹⁰⁷ Optical imaging has high sensitivity but limit to low resolution and low tissue depth penetration.¹⁰⁷ MRI has excellent resolution and no limit to tissue depth pen-

etration but suffers from low sensitivity.¹⁰⁷ Nuclear imaging techniques such as positron emission tomography (PET) and single-photon emission computed tomography (SPECT) have high sensitivity, no limit to tissue penetration but poor resolution.^{3, 107, 108} It is challenge to assess information of transplanted cells using single modality NPs. The combination of multiple modalities may provide solution to overcome the limitations of individual technique. For instance, combination of fluorescence and MRI techniques offer high sensitivity, high resolution and deep tissue penetration for labeling and tracking of cells. Several multimodal NP products are already available. Existing fluorescent and MRI dual NP products include Molday™ Rhodamine (BioPAL), iron oxide NPs with Rhodamine B (Ocean nanotech), nano-screen MAG (Chemicell). For other combinations of modalities, such as fluorescent and photoacoustic dual NPs, there is the In Vivo Plasmonic Fluorophores™ AuNPs (Nanopartz). Many other multimodal NPs are not yet commercialized but have been produced at lab scales.^{26, 69, 109-112} Although it is still at the nascent stages of the commercialization of multimodal products, the new products will provide solution for the specific limitations of single modality products and attract exceeding interests from consumers.

6.4 Limited capability to report cell viability and functions

Currently NPs can only provide temporal-spatial information and location of stem cells post transplantation.³ It would be significant to report the viability, differentiation, and even cell functions.^{3, 113} One idea is to design a smart NP with sensors, which detects stimuli associated with cell viability and functions.¹¹⁴ The stimuli includes chemicals secreted during cell differentiation, physical contact with neighboring cells during stem cell engraftment, intercellular pH changes during cell death, and certain molecules in the cell microenvironment that trigger stem cell differentiation.¹¹⁵ The identified molecular sensors will be conjugated to NPs. The interaction between the sensors and the stimuli generates detectable changes of signal in the NPs that can be captured by imaging modalities such as fluorescence or MRI. Presently NPs which can report cell viability and functions are at research and development stage and are only produced in research laboratories. No commercial NP with such capacity is available as of date. It remains challenging and takes years to develop smart NPs with reporting capacity and turn them into practical products. However, the generation of new smart NP products with a more thorough understanding of cell

viability and functions will greatly improve the applicability of NPs in stem cell tracking and provide guidance for improvement of stem cell therapy.

7. Conclusion

We summarize existing commercial NPs which can act as contrast agents for three commonly used imaging modalities for stem cell labeling and tracking. We overviewed the technology, current market status and their applications in stem cell labeling and tracking. We also discussed the concerns and limitations of existing commercial NPs and provide perspectives for the development of future NP products for stem cell therapy. Prior to the extensive use of commercial NP in stem cell therapy in humans, concerns of NPs including the unclear safety profile, signal loss in longitudinal tracking, insufficient to attain all necessary information of transplanted cells for single modality NPs and limited capability to report cell functionality and viability will have to be clearly resolved. Careful investigation of NPs effects on stem cells must be carried out prior to apply NPs in clinical trials. Micro-complex particle encapsulating multiple copies of NPs, which provides high resistance to signal dilution, can be a promising new type of product for longitudinal tracking. Multimodal NPs could out-perform single modality NPs and provide solution to attain more comprehensive information of transplanted cells. Smart NPs which can report the viability, differentiation, and cell functions would greatly advance future stem cell therapy.

Acknowledgements

We thank BioPAL Inc, MacroSpheres-MicroSpheres Inc and Chemicell Inc for providing products information. This work was supported in part by Nanyang Technological University start up Grant to XCJ.

Competing Interest

Hooisweng Ow is a Co-founder and shareholder of Hybrid Silica Technologies.

References

1. Powles R. 50 years of allogeneic bone-marrow transplantation. *Lancet.Oncol.* 2010; 11:305-6.
2. Fodor W L. Tissue engineering and cell based therapies, from the bench to the clinic: The potential to replace, repair and regenerate. *Reprod. Biol. Endocrin.* 2003; 1:102-7.
3. Xu CJ, Mu LY, Roes I, Miranda-Nieves D, Nahrendorf M, Ankrum J A, Zhao W, Karp J M. Nanoparticle-based monitoring of cell therapy. *Nanotechnology.* 2010; 22:494001-16.
4. Nguyen PK, Nag D, Wu JC. Methods to assess stem cell lineage, fate and function. *Adv Drug Deliv Rev.* 2010; 62:1175-86.
5. Rosenzweig A. Cardiac cell therapy: mixed results from mixed cells. *N. Engl. J. Med.* 2006;355: 1274-77.
6. Arbab AS, Yocum GT, Kalish H, Jordan EK, Anderson SA, Khakoo AY, Read EJ, Frank JA. Efficient magnetic cell labeling with protamine sulfate complexed to ferumoxides for cellular. *MRI.Blood.* 2004; 104:1217-23.

7. Kamaly N, Kalber T, Ahmad A, Oliver MH, So PW, Herlihy AH, Bell JD, Jorgensen MR, Miller AD. Bimodal paramagnetic and fluorescent liposomes for cellular and tumor magnetic resonance imaging. *Bioconjug Chem.* 2008;19:118-29.
8. Aime S, Barge A, Cabella C, Crich SG, Gianolio E. Targeting cells with MR imaging probes based on paramagnetic Gd(III) chelates. *Curr. Pharm. Biotechnol.* 2004; 5: 509-18.
9. Anderson SA, Lee KK, Frank JA. Gadolinium-fullerenol as a paramagnetic contrast agent for cellular imaging. *Invest.Radiol.* 2006;41:332-338.
10. Bogaards A, Sterenborg HJ, Trachtenberg J, Wilson BC, Lilge L. In vivo quantification of fluorescent molecular markers in real-time by ratio imaging for diagnostic screening and image-guided surgery. *Lasers Surg. Med.* 2007; 39:605-13.
11. Bhaumik S, Gambhir SS. Optical imaging of Renilla luciferase reporter gene expression in living mice. *Proc. Natl. Acad. Sci. USA.* 2002; 99:377-82.
12. Bulte JW, Arbab AS, Douglas T, Frank JA. Preparation of magnetically labeled cells for cell tracking by magnetic resonance imaging. *Methods Enzymol.* 2004; 386: 275-99.
13. Sheikh AY, Lin SA, Cao F, Cao Y, van der Bogt KE, Chu P, Chang CP, Contag CH, Robbins RC, Wu JC. Molecular imaging of bone marrow mononuclear cell homing and engraftment in ischemic myocardium. *Stem Cells.* 2007; 25:2677-84.
14. Ferreira L, Karp JM, Nobre L, Langer R. New opportunities: the use of nanotechnologies to manipulate and track stem cells. *Cell Stem Cell.* 2008; 3:136-46.
15. Bulte JW, Douglas T, Witwer B, Zhang SC, Strable E, Lewis BK, Zywicke H, Miller B, van Gelderen P, Moskowitz BM, Duncan ID, Frank JA. Magnetodendrimers allow endosomal magnetic labeling and in vivo tracking of stem cells. *Nat. Biotechnol.* 2001; 19:1141-47.
16. Cappello J. Overview of Nanotechnology: Risks, Initiatives and Standardization. The American society of safety Engineers.
17. [Internet] <http://en.wikipedia.org/wiki/Fluorescence>.
18. [Internet] www.abcam.com/technical.
19. Adamczyk M, Cornwell M, Huff J, Rege J, Rao T V S. Novel 7-hydroxycoumarin based fluorescent labels. *Bioorgan Med Chem Lett.* 1997; 7: 1985-88.
20. Lakowicz JR. Principles of fluorescence spectroscopy; 3rd ed. New York, USA: Springer; 2006.
21. Smith LM, Sanders ZJ, Kaiser RJ, et al. Fluorescence detection in automated DNA sequence analysis. *Nature.* 1986;321: 674 - 9.
22. Quesada MA, et al. High-sensitivity DNA detection with a laser-excited confocal fluorescence gel scanner. *Biotechniques.* 1991;10:616-25.
23. Alivisatos, AP. Semiconductor Cluster, Nanocrystals and Quantum dots. *Science.* 1996; 271: 933-7.
24. Burns A, Ow H, Wiesner U. Fluorescent core-shell silica nanoparticles: towards "lab on a particle" architectures for nanobiotechnology. *Chem. Soc. Rev.* 2006; 35: 1028-1042.
25. Muller K, Klapper M, Mullen K. Synthesis of Conjugated Polymer nanoparticles in non-aqueous emulsions. *Macromol Rapid Commun.* 2006; 27: 586-93.
26. Levitt MH. Spin Dynamics: Basics of Nuclear Magnetic Resonance. Chichester, UK: Wiley; 2008.
27. Nam SY, Ricles LM, Suggs LJ, Emelianov SY. In vivo Ultrasound and Photoacoustic Monitoring of Mesenchymal Stem Cells Labeled with Gold Nanotracers. *PLoS ONE.* 2012; 7: e37267.
28. Rossin R, Muro S, Welch MJ, Muzykantov VR, Schuster DP. In vivo imaging of Cu-64-labeled polymer nanoparticles targeted to the lung endothelium. *J. Nucl. Med.* 2008; 49: 103-11.
29. Cai W B, Chen K, Li Z B, Gambhir S S, Chen X Y. Dual-function probe for PET and near-infrared fluorescence imaging of tumor vasculature. *J. Nucl. Med.* 2007; 48: 1862-70.
30. Morales-Avila E, Ferro-Flores G, Ocampo-García BE, De León-Rodríguez LM, Santos-Cuevas CL, García-Becerra R, Medina LA, Gómez-Oliván L. Multi-meric system of 99mTc-labeled gold nanoparticles conjugated to c[RGDFK(C)] for molecular imaging of tumor $\alpha(v)\beta(3)$ expression. *Bioconjug Chem.* 2011; 22:913-22.
31. Fu CM, Wang YF, Chao YC, Hung SH, Yang MD. Labeling ferrite nanoparticles with Tc-99m radioisotope for diagnostic applications. *Magnetics, IEEE Transactions.* 2004;40: 3003-5.
32. Andrezzi E, Seo JW, Ferrara K, Louie A. Novel method to label solid lipid nanoparticles with 64Cu for positron emission tomography imaging. *Bioconjug Chem.* 2011;22: 808-18.
33. Xu CJ, Miranda-Nieves D, Ankrum JA, Matthies M E, Phillips JA, Roes I, Wojtkiewicz GR, June V, Kultima JR, Zhao W, Vermula PK, Lin CP, Nahrendorf M, Karp JM. Tracking Mesenchymal Stem Cells with Iron Oxide Nanoparticle Loaded Poly(lactide-co-glycolide) Microparticles. *Nano Lett.* 2012; 12: 4131-39.
34. Raa J P, Geckeler K E. Polymer nanoparticles: Preparation techniques and size-control parameters. *Prog. Poly. Sci.* 2011;36:887-913.
35. Wang F, Tan W, Zhang Y, Fan X, Wang M. Luminescent nanomaterials for biological labeling. *Nanotechnology.* 2006;17: R1-R13.
36. Brijmohan SB, Swier S, Weiss RA, Shaw MT. Synthesis and Characterization of Cross-linked Sulfonated Polystyrene Nanoparticles. *Ind. Eng. Chem. Res.* 2005;44: 8039-45.
37. [Internet] <http://www.distrilabparticles.com/filters/pdf/Bul120/A%20FluorPoly.pdf>.
38. [Internet] <http://www.thermoscientific.com/>.
39. [Internet] <http://www.sigmaldrich.com/life-science/biochemicals/biochemicalproducts.html?TablePage=15933819>
40. Baier, MC, Huber J, Mecking S. Fluorescent conjugated polymer nanoparticles by polymerization in mini emulsion. *J. Am. Chem. Soc.* 2009;131: 14267-73.
41. Fang L, Li Y, Wang R, Xu C, Li SH. Synthesis and photophysical properties of poly(aryleneethynylene)s bearing dialkylsilyl side substituents. *Euro. Poly. J.* 2009, 45: 1092-97.
42. Wang R, Zhang C, Wang WZ, Liu T. Preparation, morphology, and biolabeling of fluorescent nanoparticles based on conjugated polymers by emulsion polymerization. *Poly.Chem.* 2010; 48:4867-74.
43. Liu Y, Mills RC, Boncella JM, Schanze KS. Fluorescent polyacetylene thin film sensor for nitroaromatics. *Langmuir.* 2001;17: 7452-55.
44. Zhou Q, Swager TM. Fluorescent Chemosensors Based on Energy Migration in Conjugated Polymers: The Molecular Wire Approach to Increased Sensitivity. *J. Am. Chem. Soc.* 1995;117:12593-602.
45. Kleinman HK, et al. Isolation and characterization of type IV procollagen, laminin, and heparin sulfate proteoglycan from the EHS sarcoma. *Biochemistry.* 1982;21:6188-93.
46. Milovanova T, Bhopale VM, Sorokina EM, Moore JS, Hunt TK, Jensen MH, Velazquez OC, Thom S. Lactate Stimulates Vasculogenic Stem Cells via the Thioredoxin System and Engages an Autocrine Activation Loop Involving Hypoxia-Inducible Factor 1. *Mol. Cell. Bio.* 2008;28:6248-61.
47. Fujii SI, Shimizu K, Fujimoto K, Kiyokawa T, Shimomura T, Kinoshita M, Kawano F. Analysis of a Chronic Myelogenous Leukemia Patient Vaccinated with Leukemic Dendritic Cells Following Autologous Peripheral Blood Stem Cell Transplantation. *Jpn J Cancer Res.* 1999; 90: 1117-29.
48. Shimizu K, Fujii S, Fujimoto K, Kawa K, Yamada K, Kawano F. Tacrolimus (FK506) treatment of CD34+ hematopoietic progenitor cells promote the development of dendritic cells that drive CD4+ T cells toward Th2 responses. *J. Leukoc. Bio.* 2000; 68: 633-40.
49. Fujii S, Fujimoto K, Shimizu K, Ezaki T, Kawano F, Takatsuki K, Kawakita M, Matsuno K. Presentation of Tumor Antigens by Phagocytic Dendritic Cell Clusters Generated from Human CD341 Hematopoietic Progenitor Cells: Induction of Autologous Cytotoxic T Lymphocytes against Leukemic Cells in Acute Myelogenous Leukemia Patients. *Cancer Res.* 1999; 59: 2150-58.
50. Hino M, Suzuki Y, Yamane T, Sakai N, Kubota H, Koh KR, Ohta K, Hato F, Kitagawa S, Tatsumi N. Ex vivo expansion of mature human neutrophils with normal functions from purified peripheral blood CD34+ haematopoietic progenitor cells. *Br J Haematol.* 2000;109: 314-21.
51. Zhao Y, Glesne D, Huberman E. A human peripheral blood monocyte-derived subset acts as pluripotent stem cells. *Proc. Natl. Acad. Sci.* 2003; 100: 2426-31.
52. Ekimov AI, Onushchenko AA. Quantum size effect in three-dimensional microscopical semiconductor crystals. *JETP Lett.* 1981;34: 345-349.
53. Medintz I, Uyeda H, Goldman E, Mattoussi H. Quantum dot bioconjugates for imaging, labeling and sensing. *Nat. Mater.* 2005;4: 435-46.
54. Chan W.C.W, Nie S.M. Quantum Dot Bioconjugates for Ultrasensitive Nonisotopic Detection. *Science.* 1998; 285: 2016-18.
55. Yao J, et al. Blinking and nonradiant dark fraction of water-soluble quantum dots in aqueous solution. *Proc. Natl. Acad. Sci. U. S. A.* 2005;102: 14284-89.
56. [Internet] <http://www.nanotechnology.com/content/Products/CadmiumFreeQuantumDotsQFQD.aspx>.
57. Slotkin JR, Chakrabarti L, Dai HN, et al. In vivo quantum dot labeling of mammalian stem and progenitor cells. *Dev. Dynam.* 2007; 236:3393-401.
58. Stöber W, et al. Controlled growth of monodisperse silica spheres in the micron size range. *Colloid Interface Sci.* 1968; 26:62-69.
59. van Blaaderen A and Vrij A. Synthesis and characterization of monodisperse colloidal organo-silica spheres. *J. Colloid Interface Sci.* 1993;156:1-18.
60. Yamauchi, H.; Ishikawa, T.; Kondo, S. Surface Characterization of ultramicro spherical particles of silica prepared by w/o microemulsion method. *J. Colloids Surf.* 1989;37: 71-80.
61. Osseo-Asare, K.; Arriagada, F. Preparation of SiO2 nanoparticles in a non-ionic reverse micelle system. *J. Colloids Surf.* 1990; 50: 321-339.
62. Lindberg, R.; Sjöblom, J.; Sundholm, G. Preparation of silica particles utilizing the sol-gel and the emulsion-gel processes. *Colloids Surf.* A 1995;99:79-88.
63. Ow H, Larson DR, Srivastava M, Baird BA, Webb WW, Wiesner U. Bright and stable core-shell fluorescent silica nanoparticles. *Nano Lett.* 2005;5: 113-7.
64. Larson DR, Ow H, Vishwasrao HD, Heikal AA, Wiesner U, Webb WW. Silica Nanoparticle Architecture Determines Radiative Properties of Encapsulated Fluorophores. *Chem Mater.* 2008;20: 2677-84.
65. [Internet] <http://www.hybridsilica.com/c.spec-basics.html>.
66. Wang Y, Gildersleeve JC, Basu A, Zimm MB. Photo- and biophysical studies of lectin-conjugated fluorescent nanoparticles: reduced sensitivity in high density assays. *J. Phys. Chem. B.* 2010; 114: 14487-94.
67. Huang D M, Hung Y, Ko BS, Hsu SC, Chen WH, Chien CL, Tsia CP, Kuo CT, Kang JC, Yang CS, Mou CY, Chen YC. Highly efficient cellular labeling of mesoporous nanoparticles in human mesenchymal stem cells: implication for stem cell tracking. *FASEB J.* 2005;19: 2014-16.
68. Accomasso L, Cibrario Rocchietti E, Raimondo S, Catalano F, Alberto G, Giannitti A, Minieri V, Turinetto V, Orlando L, Saviozzi S, Caputo G, Geuna S, Martra G, Giachino C. Fluorescent Silica Nanoparticles Improve Optical Im-

- aging of Stem Cells Allowing Direct Discrimination between Live and Early-Stage Apoptotic Cells. *Small*. 2012; 8: 3192-200.
69. Benezra M, Medina OP, Zanzonico PB, Schaer D, Ow H, Burns A, DeStanchina E, Longo V, Herz E, Lyster S, Wolchok J, Larson SM, Wiesner U, Bradbury MS. Multimodal Silica Nanoparticles are effective cancer-targeted probes in a model of human melanoma. *J Clin Invest*. 2011; 121: 2768-80.
 70. Na BH, Song IC, Hyeon TH. Inorganic Nanoparticles for MRI Contrast Agents. *Adv. Mater.* 2009; 21: 2133-48.
 71. Laconte L, Nitin N, Bao G. Magnetic nanoparticle probes. *Mat. Today*. 2005; 8:32-38.
 72. Weinstein JS, Varallyay CG, Dosa E, Gahramanov S, Hamilton B, Rooney WD, Muldoon LL, Neuwelt EA. Superparamagnetic iron oxide nanoparticles: diagnostic magnetic resonance imaging and potential therapeutic applications in neurooncology and central nervous system inflammatory pathologies, a review. *J. Cereb. Blood Flow Metab*. 2010; 30: 15-35.
 73. Lee N, Hyeon T. Designed synthesis of uniformly sized iron oxide nanoparticles for efficient magnetic resonance imaging contrast agents. *Chem. Soc. Rev*. 2012; 41: 2575-89.
 74. Xu C J, Sun S. Superparamagnetic nanoparticles as targeted probes for diagnostic and therapeutic applications. *Dalton Trans*. 2009; 29: 5583-91.
 75. Chen M, Liu J P, Sun S. One-step synthesis of FePt nanoparticles with tunable size. *J. Am. Chem. Soc*. 2004; 126: 8394-5.
 76. Zhang XL, Wang G, Dong FR, Wang ZM. Application of magnetic resonance imaging for monitoring stem cell transplantation for the treatment of cerebral ischemia. *Neural Regen Res*. 2012; 7: 1264-71.
 77. Kowalczyk M, Banach M, Rysz J. Ferumoxytol: a new era of iron deficiency anemia treatment for patients with chronic kidney disease. *J Nephrol*. 2011;24:717-22.
 78. Bulte JW, Douglas T, Witwer B, Zhang SC, Strable E, Lewis BK, Zywicke H, Miller B, van Gelderen P, Moskowitz BM, Duncan ID, Frank JA. Magnetodendrimers allow endosomal magnetic labeling and in vivo tracking of stem cells. *Nat. Biotechnol*. 2001;19: 1141-7.
 79. Bulte JW, Duncan ID, Frank JA. In vivo magnetic resonance tracking of magnetically labeled cells after transplantation. *J. Cereb. Blood Flow Metab*. 2002; 22: 899-907.
 80. Kostura L, Kraitchman DL, Mackay AM, Pittenger MF, Bulte JW. Feridex labeling of mesenchymal stem cells inhibits chondrogenesis but not adipogenesis or osteogenesis. *NMR Biomed*. 2004; 17: 513-17.
 81. Walczak P, Bulte JWM: The Role of Noninvasive Cellular Imaging in Developing Cell-Based Therapies for Neurodegenerative Disorders. *Neurodegenerative Dis*. 2007; 4: 306-13.
 82. Liu G, Yang H, Zhang XM, Shao Y, Jiang H. MR imaging for the longevity of mesenchymal stem cells labeled with poly-L-lysine-Resovist complexes. *Contrast Media Mol Imaging*. 2010; 5: 53-8.
 83. Wang S, Zhao YG, Yan XB, Fu K, Wang LH. Migration of Resovist-labeled neural stem cells towards focal rat cerebral ischemic regions as determined by in vivo tracking and magnetic resonance imaging. *Neural Regen Res*. 2010; 5:970-74.
 84. Guo J, Shen JK, Wang L, Xiao L, Zhang RJ, Luo WF, Gong ZG, Sun J, Xu H, Sirois P, L K. In Vivo Evaluation of Cerebral Transplantation of Resovist-Labeled Bone Marrow Stromal Cells in Parkinson's Disease Rats Using Magnetic Resonance Imaging. *Appl Biochem Biotechnol*. 2011;163: 636-48.
 85. Ke YQ, Hu CC, Jiang XD, Yang ZJ, Zhang HW, Ji HM, Zhou LY, Cai YQ, Qin LS, Xu RX. In vivo magnetic resonance tracking of Feridex-labeled bone marrow-derived neural stem cells after autologous transplantation in rhesus monkey. *J Neurosci Methods*. 2009;179: 45-50.
 86. Castaneda RT, Khurana A, Khan R, Daldrup-Link HE. Labeling stem cells with ferumoxytol, an FDA-approved iron oxide nanoparticle. *J Vis Exp*. 2011;57: e3482.
 87. Gu LY. Migration of Resovist-labeled neural stem cells towards focal rat cerebral ischemic regions as determined by in vivo tracking and magnetic resonance imaging. *Neu. Regene. Res*. 2010;5:1-5.
 88. Wang YX. Superparamagnetic iron oxide based MRI contrast agents: Current status of clinical application. *Quant Imaging Med Surg*. 2011;1:35-40.
 89. Merbach AE, Toth E. The Chemistry of Contrast Agents in Medical Magnetic Resonance. New York, USA: John Wiley & Sons; 2001.
 90. [Internet] <http://www.biopal.com/images/MRI%20Product%20Price%20List.pdf>
 91. Loai Y, Ganesh T, Cheng H. Concurrent Dual Contrast for Cellular Magnetic Resonance Imaging Using Gadolinium Oxide and Iron Oxide Nanoparticles. *Intl. J. Mol. Imaging*. 2012;1155: 230942.
 92. Loai Y, Sakib N, Janik R, Foltz WD, Cheng HL. Human Aortic Endothelial Cell Labeling with Positive Contrast Gadolinium Oxide Nanoparticles for Cellular Magnetic Resonance Imaging at 7 Tesla. *Mol. Imaging*. 2012;11:166-75.
 93. Zerda A DL, Zavaleta C, Keren S, Vaithilingam S, Bodapati S, Liu Z, Levi J, Smith BR, Ma TJ, Oralkan O, Cheng Z, Chen XY, Dai HJ, Khuri-Yakub BT, Gambhir SS. Carbon nanotubes as photoacoustic molecular imaging agents in living mice. *Nature Nanotechnology*, 2008; 3: 557-62.
 94. Zerda A, Liu Z, Bodapati S, Teed R, Vaithilingam S, Khuri-Yakub BT, Chen XY, Dai HJ, Gambhir SS. Ultra-High Sensitivity Carbon Nanotube Agents for Photoacoustic Molecular Imaging in Living Mice. *Nano Lett*. 2010; 10: 2168-72.
 95. Zhang Q, Iwakuma N, Sharma P, Moudgil BM, Wu C, McNeill J, Jiang H, Grobmyer SR. Gold nanoparticles as a contrast agent for in vivo tumor imaging with photoacoustic tomography. *Nanotechnology*. 2009; 20: 395102.
 96. Nam SY, Sokolov K, Emelianov SY, Suggs LJ, Ricles LM. Function of mesenchymal stem cells following loading of gold nanotracers. *Intl. J. Nanomedicine*. 2011;6: 407-16.
 97. Menk RH, Schültke E, Hall C, Arfelli F, Astolfo A, Rigon L, Round A, Atefmann K, MacDonald SR, Juurlink BH. Gold nanoparticle labeling of cells is a sensitive method to investigate cell distribution and migration in animal models of human disease. *Nanomedicine*. 2011; 5:647-54.
 98. Jokerst JV, Thangaraj M, Kempen PJ, Sinclair R, Gambhir SS. Photoacoustic Imaging of Mesenchymal Stem Cells in Living Mice via Silica-Coated Gold Nanorods. *ACS Nano*, 2012;6: 5920-30.
 99. Ferreira, L, Karp JM, Nobre L, Langer R. New opportunities: The use of nanotechnologies to manipulate and track stem cells. *Cell Stem Cell*. 2008; 3:136-146.
 100. Chang YK, Liu YP, Ho JH, Hsu SC, Lee OK. Amine-surface-modified superparamagnetic iron oxide nanoparticles interfere with differentiation of human mesenchymal stem cells. *J Orthop Res*. 2012;9: 1499-506.
 101. Ramaswamy S, Greco JB, Uluer MC, Zhang ZJ, Zhang ZL, Dishbein KW, Spencer RG. Magnetic Resonance Imaging of Chondrocytes Labeled with Superparamagnetic Iron Oxide Nanoparticles in Tissue-Engineered Cartilage. *Blood*. 2004; 104: 3410-2.
 102. Bulte JW, Kraitchman DL, Mackay AM, Pittenger MF. Chondrogenic differentiation of mesenchymal stem cells is inhibited after magnetic labeling with ferumoxides. *Tissue Eng Part A*. 2009; 15: 3899-3910.
 103. Kraitchman DL, Gilson WD, Lorenz CH. Stem cell therapy: MRI guidance and monitoring. *J. Magn. Reson. IM*. 2008; 27: 299-310.
 104. Cromer Berman S M, Walczak P, Bulte J W M. Tracking stem cells using magnetic nanoparticles. *Nanomed. Nanobiotechnol*. 2011; 3: 343-55.
 105. Neri M, Maderna C, Cavazzin C, Deidda-Vigoriti V, Politi LS, Scotti G, Marzola P, Sbarbati A, Vescovi A, Gritti A. Efficient in vitro labeling of human precursor cells with superparamagnetic iron oxide particles: relevance for in vivo cell tracking. *Stem Cells*. 2008, 26:505-16.
 106. Tovmachenko OG, Graf C, van den Heuvel DJ, van Blaaderen A, and Gerritsen HC. Fluorescence Enhancement by Metal-Core/Silica-Shell Nanoparticles. *Adv. Mater*. 2006;18: 91-95.
 107. Minchin RF, Martin DJ. Minireview: Nanoparticles for Molecular Imaging—An Overview. *Endocrinology*. 2010;151:474-81.
 108. Jennings LE, Long NJ. Two is better than one—probes for dual-modality molecular imaging. *Chem Commun*. 2009;24:3511-24.
 109. Mulder WJ, Koole R, Brandwijk RJ, Storm G, Chin PT, Strijkers GJ, de Mello Donega C, Nicolay K, Griffioen AW. Quantum dots with a paramagnetic coating as a bimodal molecular imaging probe. *Nano Lett*. 2006; 6:1-6.
 110. Veisoh O, Sun C, Gunn J, Kohler N, Gabikian P, Lee D, Bhattarai N, Ellenbogen R, Sze R, Hallahan A, Olson J, Zhang M. Optical and MRI multifunctional nanoprobe for targeting gliomas. *Nano Lett*. 2005;5:1003-8.
 111. Koole R, Schooneveld MM, Hilhorst J, Castermans K, Cormode DP, Strijkers GJ, Donega CM, Vanmaekelbergh D, Griffioen AJ, Nicolay K, Fayad ZA, Meijerink A, Mulder J WM. Paramagnetic Lipid-Coated Silica Nanoparticles with a Fluorescent Quantum Dot Core: A New Contrast Agent Platform for Multimodality Imaging. *Bioconjugate Chem*. 2008; 19: 2471-79.
 112. Ghica C, Ionita P. Paramagnetic silica-coated gold nanoparticles. *J. Mater. Sci*. 2007; 24:10058-64.
 113. Zhang S, Wu J C. Comparison of imaging techniques for tracking cardiac stem cell therapy. *J. Nucl. Med*. 2007;48:1916-19.
 114. Zhao W, Schafer S, Choi J, Yamanaka YJ, Lombardi ML, Bose S, Carlson A, Philips JA, Tao WS, Droujinine IA, Cui CH, Jain RK, Lammerding J, Love JC, Lin CP, Sarkar D, Karnik R, Karp JM. Cell-surface sensors for real-time probing of cellular environments. *Nature. Nanotech*. 2011; 6: 524-531.
 115. [Internet] <http://stemcells.nih.gov/info/basics/basics2.asp>.
 116. [Internet] <http://www.clinicaltrials.gov>.